Paper No.
50

CORROSION 98

CALCULATION OF MASS TRANSFER IN MULTIPHASE FLOW

L. JIANG, M. GOPAL
NSF, I/UCRC CORROSION IN MULTIPHASE SYSTEMS CENTER
DEPARTMENT OF CHEMICAL ENGINEERING
OHIO UNIVERSITY, ATHENS, OHIO, USA

ABSTRACT

This paper summarizes the results of mass transfer mechanisms under disturbed liquid-gas flow in 10 cm diameter pipe using electrochemical limiting current density and potentiostatic noise technique. The solution used is potassium ferro/ferricyanide dissolve in 1.3 N sodium hydroxide system. Mass transfer coefficients in full pipe flow and slug flow are obtained. The relationship between mass transfer coefficient with full pipe flow velocities and with slug flow Froude numbers are studied. The impact of bubbles in slugs on the mass transfer coefficient is revealed. The impact of flow disturbance, including weld beads and pits, are discussed for both full pipe flow and slug flow.

Keywords: **full pipe flow, slug flow, disturbed flow, mass transfer, limiting current method, polarization, corrosion.**

INTRODUCTION

Slug flow exists in the pipelines at high production rate of oil and gas. High velocity slugs are very turbulent and the corrosion rate is increased greatly in this flow regime. This is due to pulses of gas bubbles entrained in the mixing zone being forced towards the bottom of the pipe. There they impact and can collapse, causing localized corrosion.

Further, severe corrosion is found in the vicinity of flow disturbances such as weld beads, pits, and pipe connections. This is thought to be due to the enhanced turbulence and mass transfer rate around such obstacles. No information exists at the present time regarding the mass transfer mechanisms under disturbed flow conditions.

It has been found that the corrosion rate is strongly related to the mass transfer rate of corrosive ions in the multiphase mixture from the bulk to the pipe wall. It is suggested that the mass transfer coefficient is the main parameter in the corrosion modeling (Zhang et al., 1997). However, the mass transfer coefficients in large diameter pipe flow and in multiphase flow are not known. It would be very helpful to measure mass transfer coefficients for multiphase flow systems of interest in oil and gas production.

Mass transfer measurements using limiting current method provide a convenient and accurate means to determine the local mass transfer coefficient. Small insulated electrodes embedded in flow pipe wall could provide local mass transfer coefficients. Due to their fast response, instantaneous fluctuating values, which directly reveal the local turbulence could be obtained by potentiostatic current noise measurement.

Reiss (1962) described in detail, the technique of making measurements of mass transfer using a diffusion controlled electrolytic reaction, and the use of this technique to measure velocity fluctuations at the wall. Measurements of mass transfer coefficient and intensity were carried out in 2.54 cm diameter pipe using the potassium ferro-ferricyanide electrochemical system. The electrodes were made from three sizes of nickel wire (1.636 mm, 0.664 mm, 0.397 mm in diameter respectively).

Shaw and Hanratty (1964) measured local time average mass transfer coefficients with embedded test electrode. Their experiment differed from that of Reiss in that the test electrodes, instead of being surrounded by inert surface, are surrounded by active electrode surface. Test electrodes of four different diameter were used. They found the very large magnitude of the fluctuations in the mass transfer rate (mass transfer intensity is as much as 0.47), the relative sizes of the longitudinal and circumferential scales, and the low frequency scales of mass transfer fluctuations.

Sirkar and Hanratty (1970) obtained the root-mean-square fluctuating mass transfer coefficient for a Schmidt number of about 2300 in a 7.62 cm diameter pipe. They used order-of-magnitude analysis and concluded that flow fluctuations in the direction of mean flow have little effect on the mass transfer fluctuations. The local value of mass transfer coefficient they obtained is more accurate compared with Shaw & Hanratty.

Mizushina (1971) discussed the method of diffusion-controlled electrochemical reaction and its applications in the study of transport phenomena, including mass transfer measurements, shear stress measurements and fluid velocity measurements. He also provides a review emphasizing the application of limiting current measurements on microelectrodes for local and instantaneous shear stress and velocity determinations, as described by Hanratty (1966).

Selman and Tobias (1978) compiled over a hundred mass transport correlations pertaining to different transport, flow, and agitation configurations. The theory and practice of limiting-current technique for the measurement of mass-transport coefficients were described.

Landau (1981) used limiting current technique to determine the mass transport rates of laminar and turbulent flows. He also discussed the consideration of current distribution, selection and placement of the electrodes, modes of current application and the electrochemical system selected.

Campbell and Hanratty (1983) studied the structure of the velocity field close to a wall by measuring the transverse component of the fluctuating velocity gradient simultaneously at multiple locations on the wall. Velocity fluctuations of all frequencies appear to have the same transverse scale. Measurement were held in 8 inches pipe system. It is found that frequency spectra and intensities are universal properties and not strongly affected by the particular design of the experimental flow system.

Mass transfer coefficient is calculated from the average limiting current using the following equation:

$$K = I_L / (n F A C_b) \qquad (1)$$

where K = mass transfer coefficient
I_L = limiting current
n = number of moles reacted
F = Faraday's constant
A = surface area of the electrode
C_b = bulk concentration of the potassium ferrocyanide

Mass transfer deviation is calculated from the potential static noise curve using the following equation:

$$Dev_K = [\Sigma(k - Avg_k)^2/N]^{1/2} \qquad (2)$$

where Dev_K = mass transfer deviation
k = instantaneous mass transfer coefficient
Avg_k = mean value of the instantaneous mass transfer coefficients
N = total number of the instantaneous mass transfer coefficients

EXPERIMENTAL SETUP

The overall layout of the system is shown in Figure 1. The flow loop is a 10 m long 10 cm in diameter Plexiglass pipe. A 1 m^3 stainless steel tank is filled with 1.3 N sodium hydroxide and 0.01 M potassium ferricyanide/ferrocyanide. Nitrogen is stored in a pressured gas tank and is added into the system through a pressurized regulator and a needle valve.

The test section is a 10 cm diameter Plexiglas pipe with electrodes and disturbance block. The orientation of the electrodes in the direction of flow are as follows: the reference electrode, disturbance block, working electrode and counter electrode. The overall layout of it is shown in Figure 2. The disturbance block simulates the disturbance inside a pipe line, such as weld bead and pits. The weld bead is a small hump. The pit is a small cylinder hole. The counter electrode is a ring electrode mounted flush with the pipe wall. The working and reference electrodes are hastalloy pins inserted in the Plexiglass block, laying out equal-distantly in a line at the bottom of the pipe. The distance between two consecutive electrodes is 4.5 mm and the surface area of it is 7.85×10^{-7} square meter. The dimensions of the weld beads and the pits are described in Table 1 and 2.

The data were taken by Gamry software CMS 100 installed in a Pentium computer. Two types of results were collected. The first was the DC polarization curve, from which the anodic limiting current was determined. The other was electrochemical current noise curve that was measured by setting the potential value at which the limiting current was reached.

Table 1. The Dimension of the Weld Bead Test Section

Test Section	1 mm Weld Bead	2 mm Weld Bead
Height (mm)	1	2

Table 2. The Dimension of the Pit Test Section

Test Section	Pit #1	Pit #2	Pit #3	Pit #4	Pit #5	Pit #6
Diameter (mm)	2	4	2	4	2	4
Depth (mm)	2	2	4	4	6	6

EXPERIMENTAL TEST MATRIX

Full pipe flow and slug flow experiments were conducted for the ferro/ferricyanide system. In order to study the effect of disturbance resource, nine test sections were studied at three different velocities. Table 3 showed the Experiments carried out.

Table 3. Experimental Test Matrix

Flow Velocity (for full pipe flow, m/s)	0.5, 1, 2
Froude Number (for slug flow)	4, 6, 9
Test Section	2 Weld Bead, 6 Pit, 1 Smooth Section
Electrode	1, 2, 3, 4, 5

RESULTS AND DISCUSSION

Full Pipe Flow Results

The results of smooth test section, pit #1 and 2 mm weld bead section are shown in Figure 3. When the flow velocity is 0.5 m/s, the average mass transfer coefficients in these three test sections are 0.83×10^{-4} m/s, 0.96×10^{-4} m/s and 1.00×10^{-4} m/s respectively. As the flow velocity increases to 2.0 m/s, the mass transfer coefficients increase to 1.72×10^{-4} m/s, 2.43×10^{-4} m/s and 3.12×10^{-4} m/s respectively. It is seen that the mass transfer coefficients increase with increase of full pipe flow velocity in disturbed and undisturbed flow. At the same flow velocity, such as 1m/s, the mass transfer coefficients of the Pit #1 section and 2 mm weld bead are 1.51×10^{-4} m/s and 1.79×10^{-4} m/s, both being higher than the mass transfer coefficient of smooth section which is 1.17×10^{-4} m/s. This is due to the enhanced turbulence causing by the disturbance inside the pipe. As the flow velocity increases, the mass transfer coefficients in disturbed flow increase faster than those in undisturbed flow.

In Figure 4, the mass transfer coefficients for 1 mm weld bead and 2 mm weld bead test section are compared. For 1 mm weld bead, the mass transfer coefficient at the first electrode, which is the nearest one to the weld bead, is 2.59×10^{-4} m/s. It increases to 3.68×10^{-4} m/s at the second electrode. Then it decreases to 3.15×10^{-4} m/s at the third electrode and slightly increase to 3.31×10^{-4} m/s at the fifth electrode. For 2 mm weld bead, the mass transfer coefficient at the first electrode is 1.99×10^{-4} m/s, lower than 1 mm weld bead. It increases to 3.44×10^{-4} m/s and 3.49×10^{-4} m/s at the second and third electrode, slightly higher than 1 mm weld bead at third electrode. Then it decreases to 2.86×10^{-4} m/s at the fifth electrode. This can be explained by the flow structures affected by the weld bead. The weld bead acts as a bump causing more to the downstream and forms a relatively quiescent area next to the weld bead. In this quiescent area, the flow velocity is relatively low and so on the mass transfer coefficient. The higher the weld bead, the longer it takes for the flow to redevelop. The maximum mass transfer coefficient appears at the point where the turbulent eddy hits the bottom of the pipe after flowing over the weld bead. For 1 mm weld bead, this occurs near the second electrode, whereas for 2 mm weld bead, this occurs downstream the third electrode, where they reach the highest mass transfer coefficient.

Mass transfer coefficients in Pit #1 and Pit #6 are compared in Figure 5 For Pit #1, it is seen that the mass transfer coefficient at the first electrode, which is located at the bottom of the pit, is 0.005×10^{-4} m/s, much lower than the values of other electrodes. Pit #1 is the smallest pit in our experiments, and the turbulent flow can not reach the bottom of the pit. Therefore, the liquid inside the pit is stagnant, causing the mass transfer coefficient to decrease to extremely low value. The K value greatly increases to 1.33×10^{-4} m/s at the second electrode and then slightly increases to 1.47×10^{-4} m/s at the fifth one. For Pit #6, the mass transfer coefficient at the first electrode is 0.89×10^{-4} m/s, much higher than Pit #1. This is due to the large size of Pit #6, because flow is more turbulent in the large pit than in the small one. The mass transfer coefficient increases to 1.82×10^{-4} m/s at the second electrode and slightly decreases to 1.76×10^{-4} m/s at the fifth one. These results show that the larger pit causes more turbulent down stream, than the smaller one and results in higher mass transfer coefficient.

Figure 6 shows the mass transfer deviations of 2 mm weld bead at different full pipe flow velocity. At velocity of 2.0 m/s, the mass transfer deviation for the first electrode is 1.24×10^{-5} m/s. It increases to 1.71×10^{-5} m/s at the second electrode and decreases to 1.03×10^{-5} m/s at the fifth electrode. It has the similar trend as mass transfer coefficient in Figure 4. The value of mass transfer deviation is about 3%~4% of the value of mass transfer coefficient. The other test sections have the similar results.

Slug Flow Results

Figures 7 to 11 reveal very unique instantaneous fluctuations in slug flow. These are plots of electrochemical noise. In Figure 7, smooth section, at Froude number 6, it is seen that at time instants of 0.3, 0.75 & 1.0 s, the instantaneous fluctuation is 2.4×10^{-3} m/s, 10 times higher than the average value.

In Figure 8, smooth section, Froude number 9, there are peaks of 2 different magnitudes. At 0.65 s, the peaks are 10 times higher than the mean. At 0.8, 1.2 & 1.5 s, several huge peaks appear, which are 100 times higher than the mean.

These are related to the pulses of gas bubbles reaching the electrode surface. When the slug approaches close to the electrode, the bubbles are forced down towards the surface of the pipe wall, and do impact, causing mass transfer coefficient to increase such values.

At these higher Froude numbers, the impact of bubbles on the pipe surface causes the mass transfer coefficient to increase dramatically by about 100 times. These unique mechanisms can explain the occurrence of severe localized corrosion in slug flow.

Figures 9-11 are the results of Pit #1. Figure 9 is shown for Froude number 4. The results are similar to those shown before. For example, at time instants of 0.4, 0.7, 0.9 & 1.75 s, peaks about 10 times the average occur, which indicate that the instantaneous mass transfer coefficient at this time is about 2.4×10^{-3} m/s. Figure 10 shows that for Froude number 6, in addition several peaks which are 10 times greater than the average, two peaks 100 times the average appear and the value is 2.0×10^{-2} m/s. In Figure 11, at Froude number 9, most peaks are indicate that the instantaneous mass transfer coefficients at this time are about 2.3×10^{-2} m/s, 90-100 times higher than the average.

The results of weld beads are similar to the results of pits.

For smooth section, no peak appears at Froude number 4, while at Froude number 6, peaks are only 10 times the average, and at Froude number 9, a few peaks are 100 times high. For disturbed sections, peaks of 10 times the average appear at Froude number 4, at Froude number 9, most peaks are 100 times high. It shows that disturbed flow is more turbulent than undisturbed flow.

CONCLUSION

The limiting current density technique has been demonstrated in multiphase flows for measuring mass transfer mechanisms using potassium ferro/ferricyanide dissolved in 1.3N sodium hydroxide.

In full pipe flow, mass transfer coefficient increases with full pipe velocity. For the same flow velocity, mass transfer coefficient in disturbed flow is higher than that in undisturbed flow. For weld bead, the minimum mass transfer coefficient is reached at the first electrode, which is next to the weld bead, due to decrease in turbulence. The maximum mass transfer rate locates at the end of this quiescent zone, between the second and the third electrode. The higher the weld bead dimensions, the longer the quiescent zone. For pit, the minimum mass transfer coefficient appears at the bottom of the pit. Other downstream locations experience high values of mass transfer rate. Larger pit creates more turbulent than smaller ones.

In slug flow, average mass transfer coefficients increase with Froude number. At a Froude number of 6, instantaneous increases in mass transfer coefficient, about 10 times the average value, are seen. These are due to the turbulence of gas bubbles in the mixing zone. At a higher Froude number of 9, there are still peaks 10 times the average, but now peaks 100 times the average are seen. These are caused by the actual impact of pulses of bubbles on the electrode surface. It is found that instantaneous averages in slug flow can be 1-2 orders of magnitude higher in the mixing zone compared to stratified or full pipe flow, resulting in highly increased corrosion rate. For the same Froude number, disturbed flow is more turbulent than undisturbed flow, while the size of disturbance does not cause much effect on it.

REFERENCE

1. Campbell, J. A. and Hanratty, T. J. (1983). "Mechanism of Turbulent Mass Transfer at a Solid Boundary", A.I.Ch.E. Journal, 29,221

2. Landau, U. (1981). "Determination of Laminar and Turbulent Mass Transport Rates in Flow Cells by the Limiting Current Technique", Ph.D. Thesis, Case Western Reserve University, Cleveland

3. Mizushina, T., Irvine, T. F., and Hartnett, J. P. (1971). Academic Press 7

4. Reiss, L. P. (1962). "Investigation of Turbulence Near a Pipe Wall Using a Diffusion Controlled Electrolytic Reaction on a Circular", Ph.D. Thesis, University of Illinois, Urbana

5. Selman, J. R. and Tobias, C. W., (1978) " Limiting-Current Mass-Transfer Measurements", Advances in Chemical Engineering, Vol. 11, No. 3, pp. 271

6. Shaw, P. V. and Hanratty T. J. (1964). "Fluctuations in the Local Rate of Turbulent Mass Transfer to a Pipe Wall", A.I.Ch.E. Journal, 10, 475

7. Sirkar, K. K. and Hanratty, T. J. (1970). "Relation of turbulent mass transfer to a wall at high Schmidt numbers to the velocity field", J. Fluid Mech., 44, 589

8. Zhang, R., Gopal, M. and Jepson, W. P. (1997). "Development of a Mechanistic Model for Predicting Corrosion Rate in Multiphase Oil/Water/Gas Flows", CORROSION/97, Paper No. 601

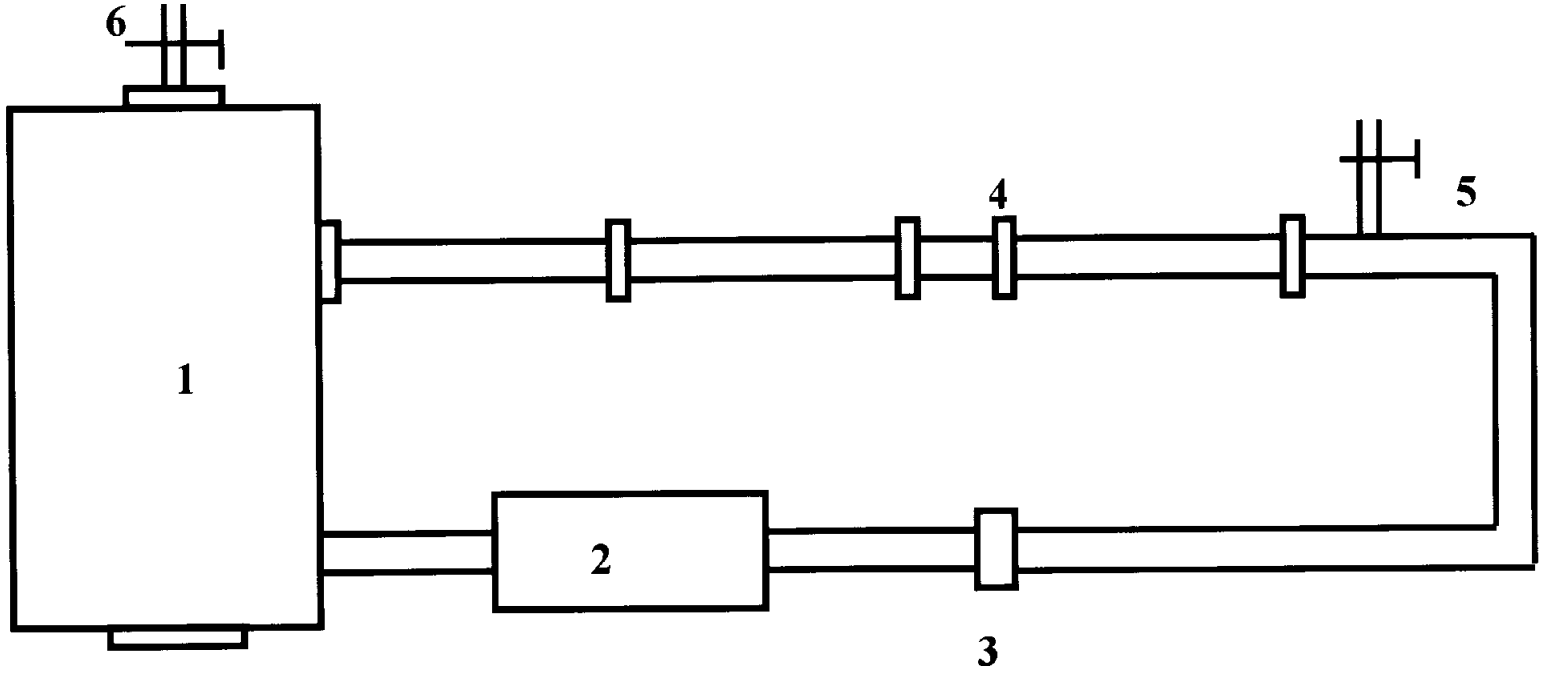

1. Tank
2. Pump
3. Orifice Plate, Pressure Transducer
4. Test Section
5. Gas Fed in
6. Gas Vented

Figure 1. System Layout

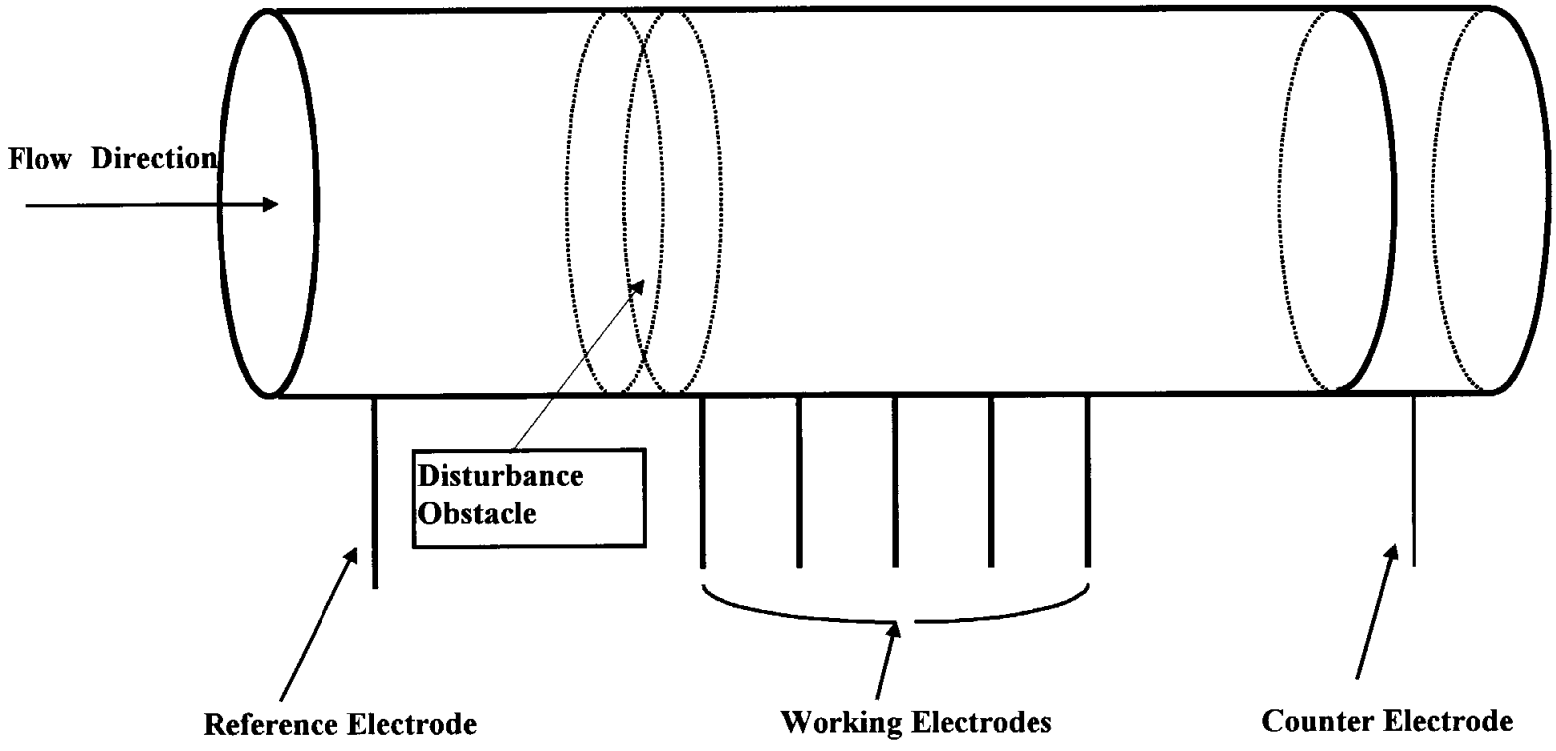

Figure 2. Test Section Layout

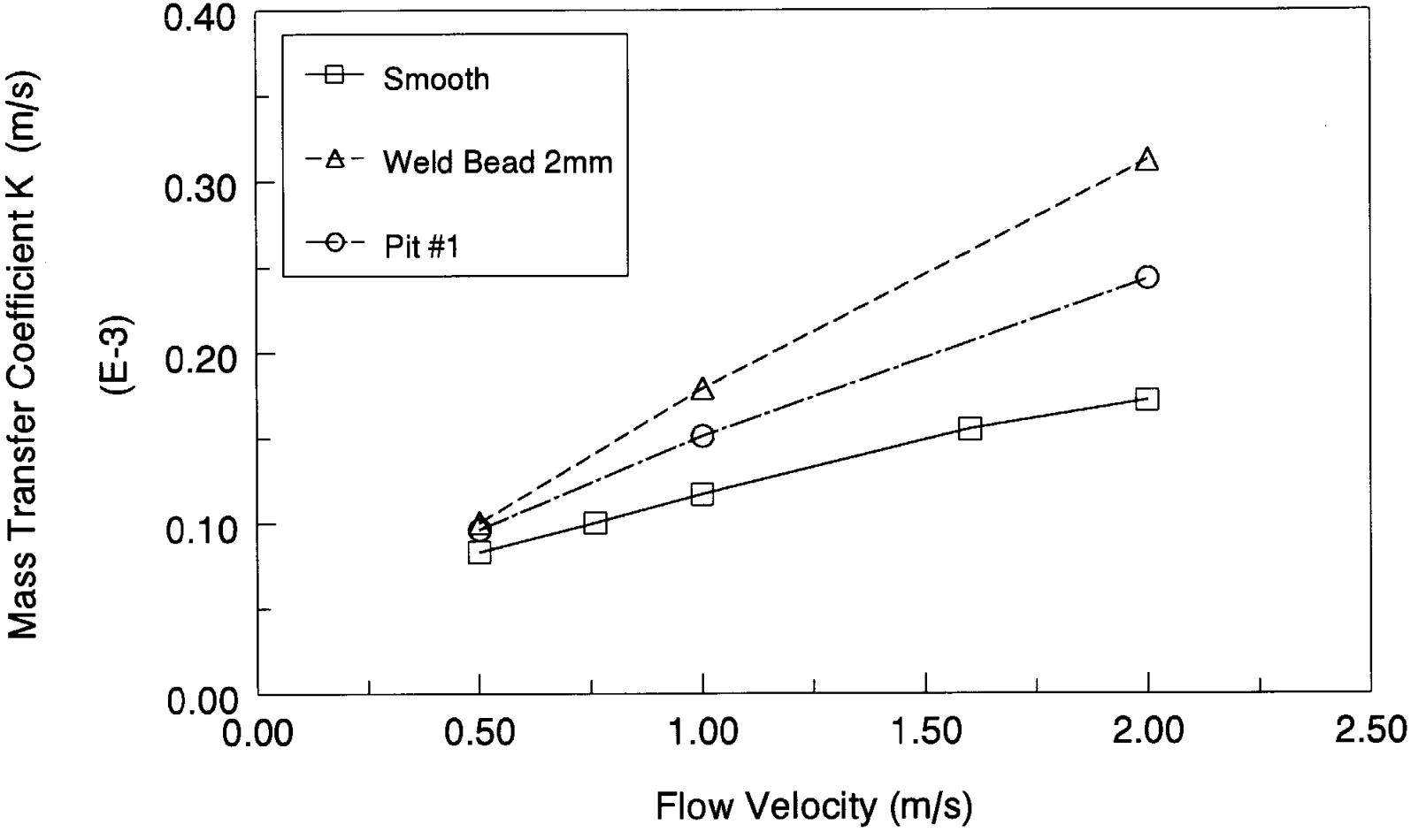

Figure 3. Mass Transfer Coefficient vs. Full Pipe Flow Velocity in Smooth Section, Weld Bead 2mm and Pit #1 electrode #4

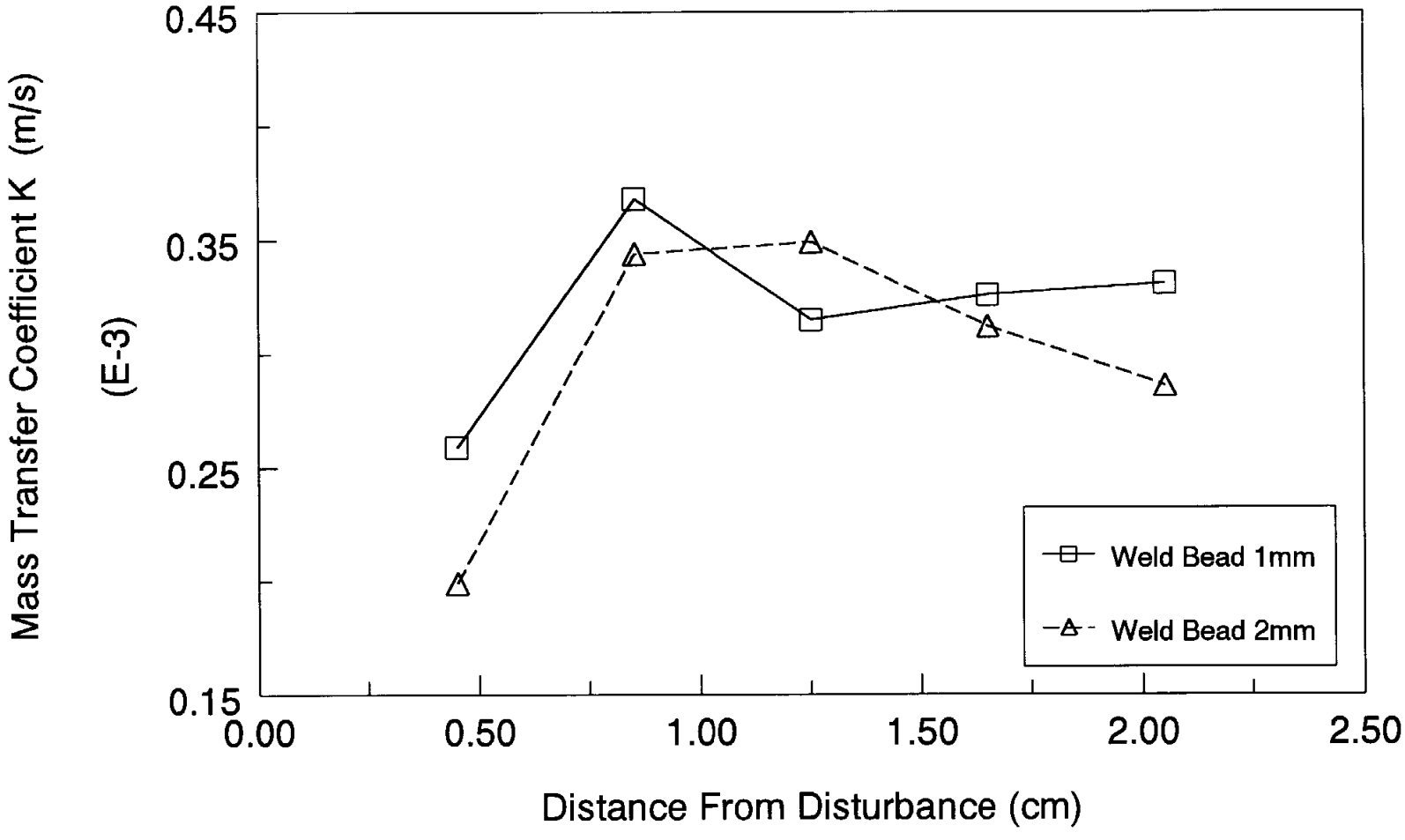

Figure 4. Mass Transfer Coefficient vs. Distance From Disturbance in Full Pipe Flow for Weld Bead 1mm and 2mm Velocity 2m/s

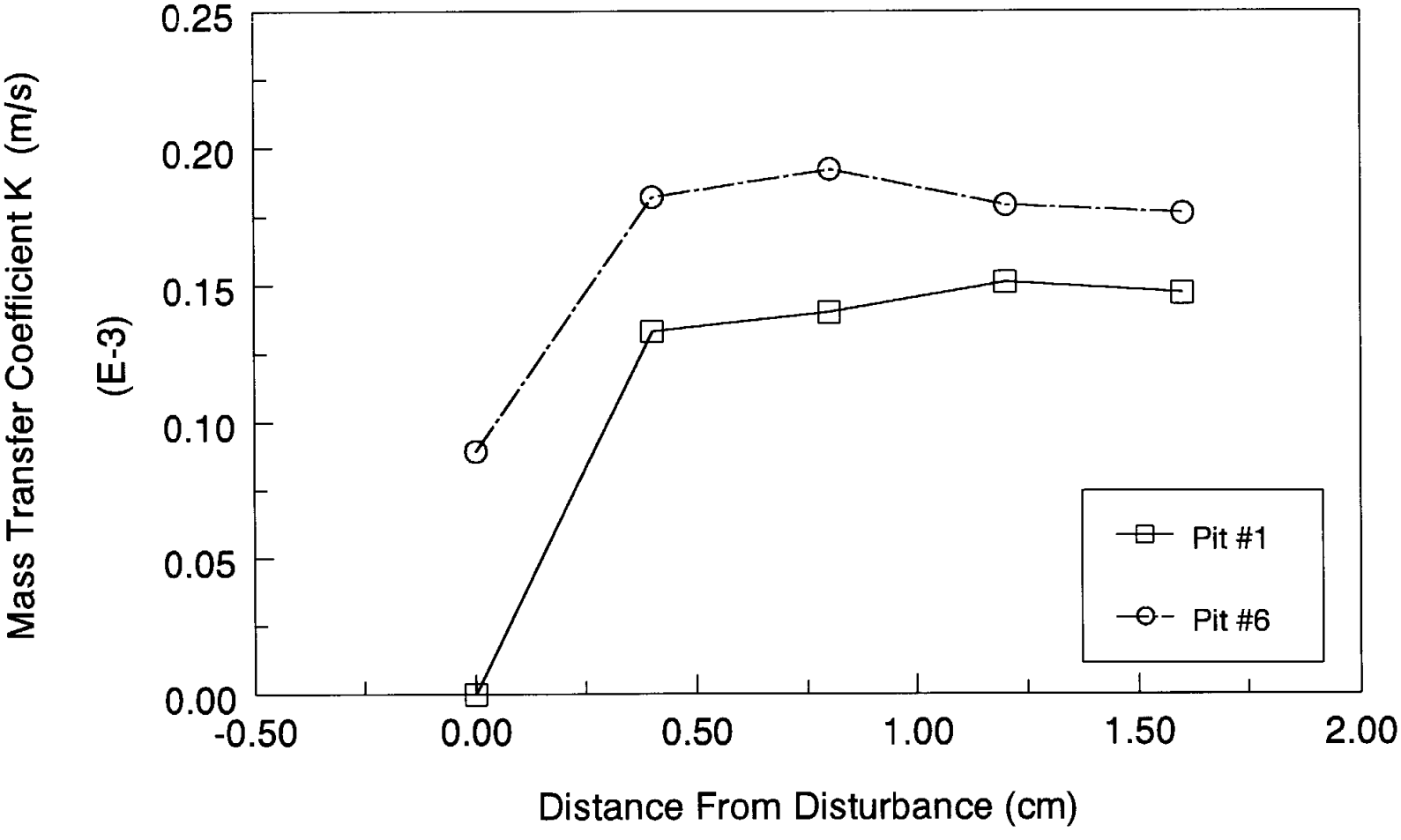

Figure 5. Mass Transfer Coefficient vs. Distance From Disturbance in Full Pipe Flow for Pit #1 and Pit #6 at Velocity 1m/s

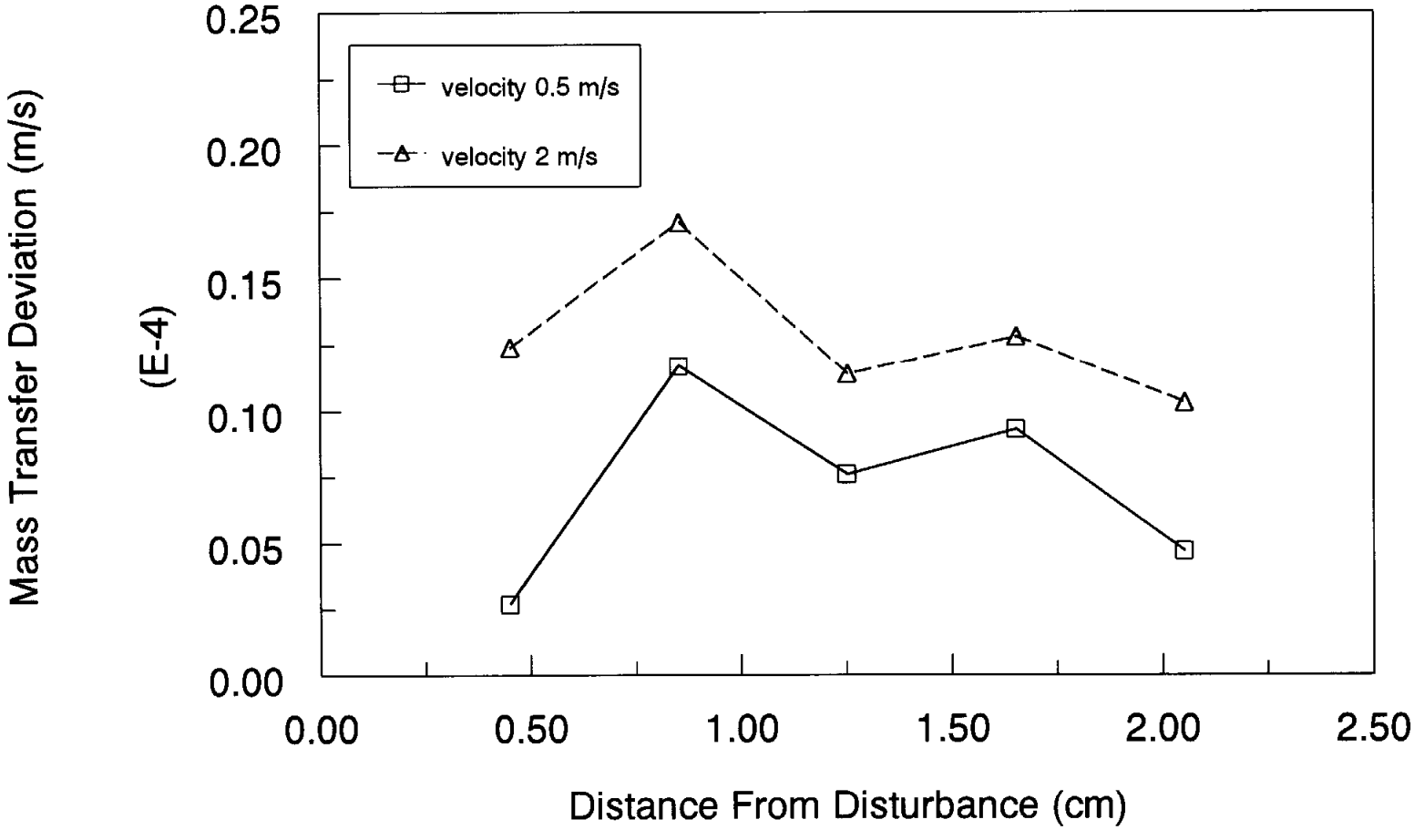

Figure 6. Mass Transfer Deviation vs. Distance From Disturbance for Weld Bead 2 mm at Velocity 0.5 m/s and 2 m/s in Full Pipe Flow

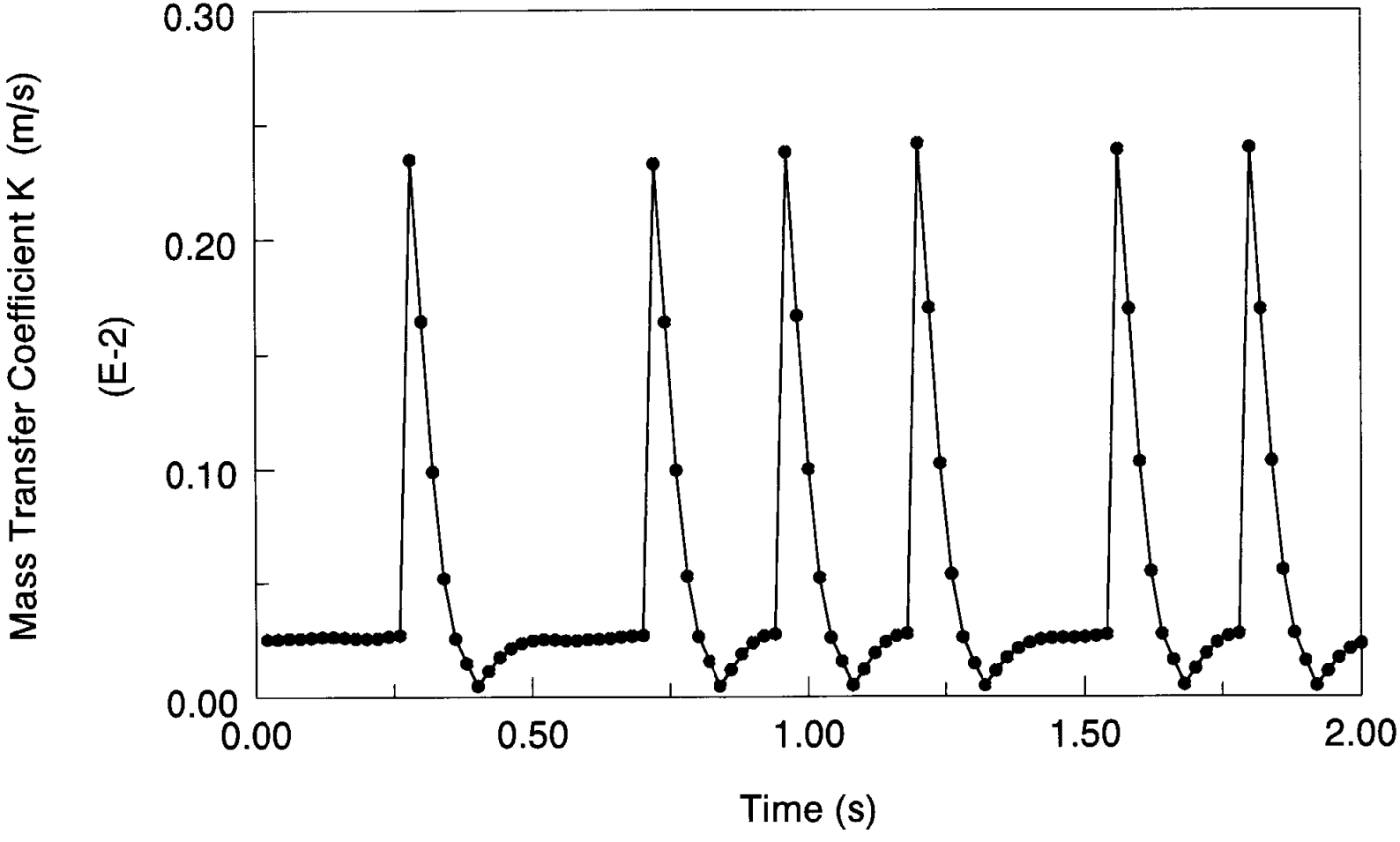

Figure 7. Instantaneous Mass Transfer Coefficient vs. Time for Smooth Section at Froude Number 6

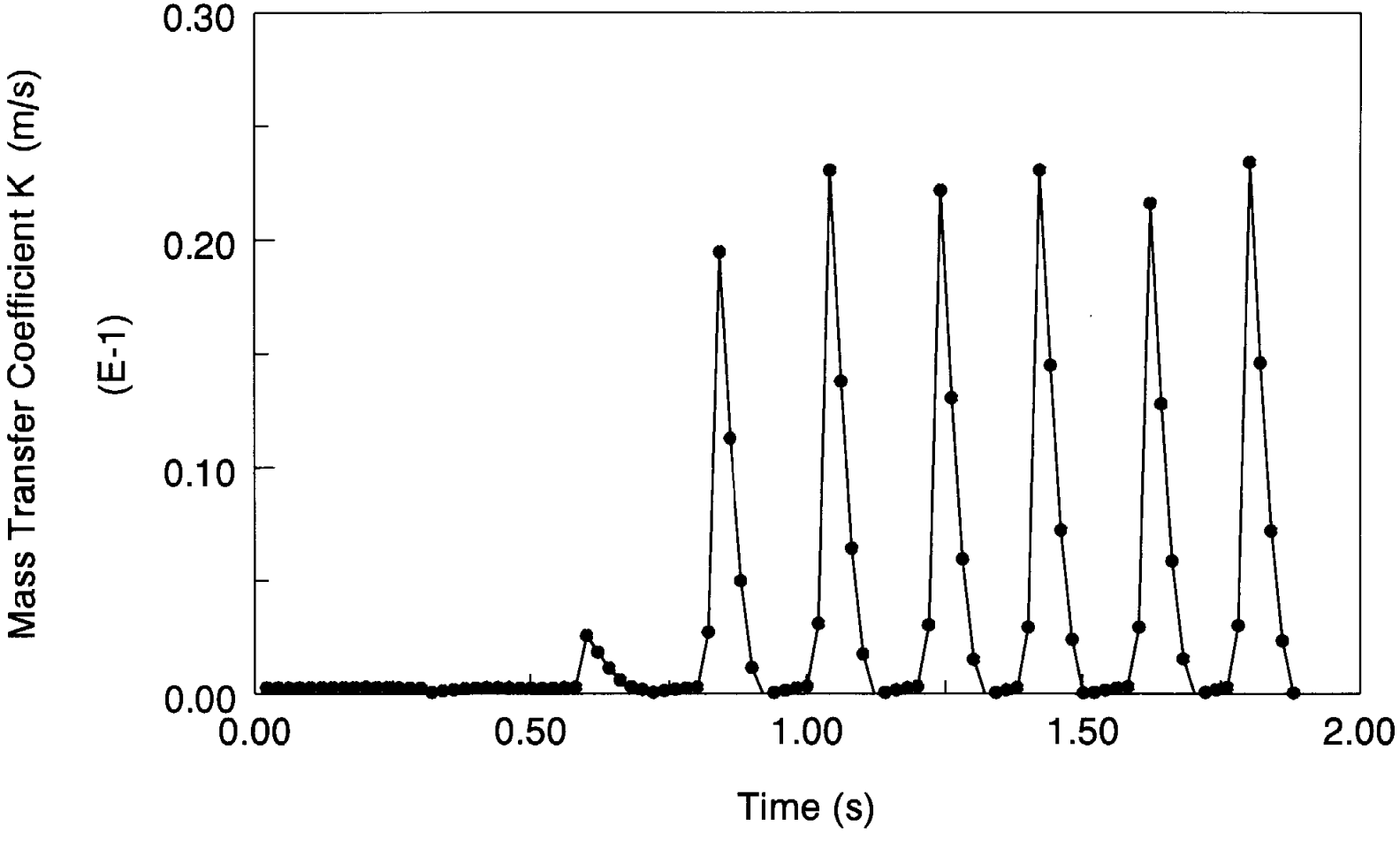

Figure 8. Instantaneous Mass Transfer Coefficient vs. Time for Smooth Section at Froude Number 9

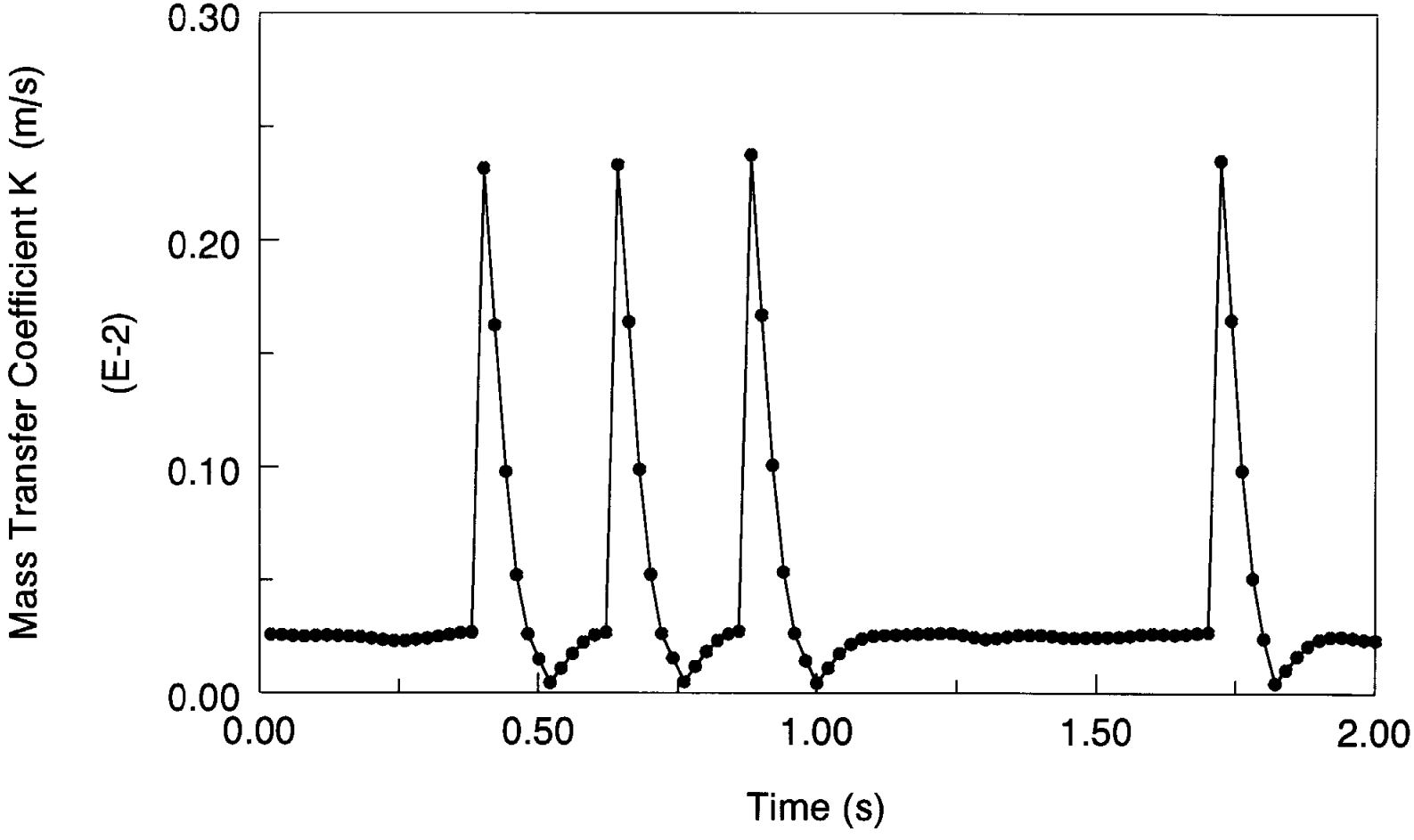

Figure 9. Instantaneous Mass Transfer Coefficient vs. Time
for Pit #1 at Froude Number 4
electrode 4

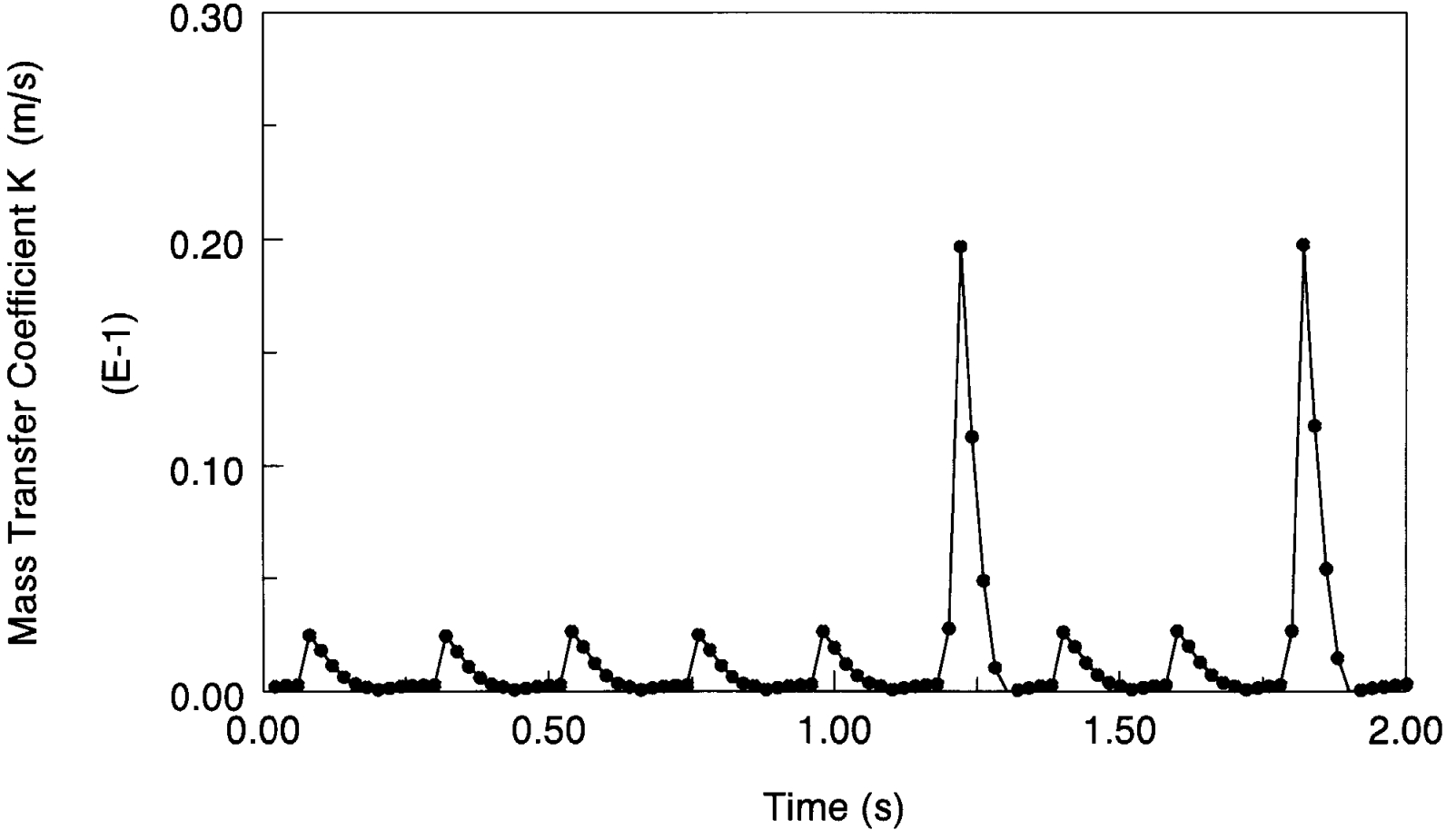

Figure 10. Instantaneous Mass Transfer Coefficient vs. Time
for Pit #1 at Froude Number 6
electrode 4

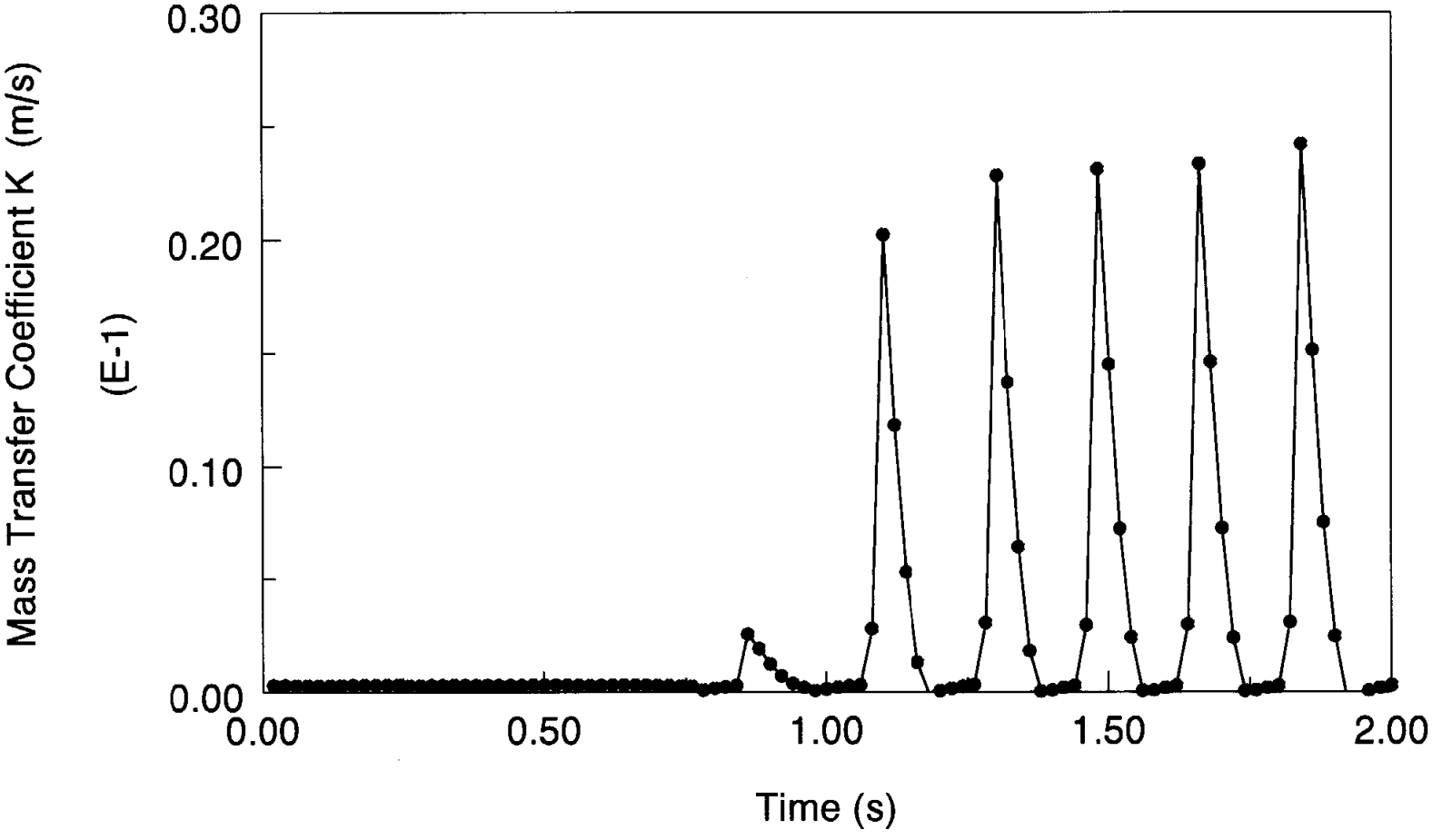

Figure 11. Instantaneous Mass Transfer Coefficient vs. Time
for Pit #1 at Froude Number 9
electrode 4